IEEE Access
Multidisciplinary | Rapid Review | Open Access Journal

Received January 28, 2020, accepted February 13, 2020, date of publication February 17, 2020, date of current version February 27, 2020.

Digital Object Identifier 10.1109/ACCESS.2020.2974405

Low-Cost and High-Efficiency Method for Detecting Vertical Bends of Subsea Pipelines

GUO LIN, ZENG ZHOUMO, HUANG XINJING, LI MINGZE, FENG HAO, LI JIAN, AND RUI XIAOBO

State Key Laboratory of Precision Measuring Technology and Instruments, Tianjin University, Tianjin 300072, China
Binhai International Advanced Structural Integrity Research Centre, Tianjin University, Tianjin 300072, China

Corresponding author: Huang Xinjing (huangxinjing@tju.edu.cn)

This work was supported in part by the National Natural Science Foundation of China under Grant 51604192, Grant 61773283, and Grant 61973227, and in part by the China Postdoctoral Science Foundation under Grant 2018M630271.

ABSTRACT Subsea pipelines often bend upward due to vertical buckling or downward due to spanning and seabed settling. Typically, harsh environments and the difficulty of accessing underwater pipelines make the inspection and monitoring of subsea pipeline bends a challenging task. This paper demonstrates a low-cost, high-efficiency, and quasi-real-time method for detecting the vertical bends of subsea pipelines by using an in-pipe spherical detector (SD) with rolling features and a low blockage risk. When the SD rolls forward inside a bent pipeline, its rolling speed will change as it moves uphill and downhill, which can be indicated by the centripetal acceleration—the DC component of the recorded rolling acceleration signals. To achieve a high bend detection performance, the mass of the SD should be distributed in a centered disc area to make the SD capable of stably rolling around one of the sensitive axes of the accelerometer, and the accelerometer should be kept as far from the rotation axis as possible. It is experimentally demonstrated that a convex/concave DC component indicates that the pipe is bent downward/upward, and the bend detection resolution can reach 1 cm for a 12 m pipeline.

INDEX TERMS Subsea pipeline, spanning, buckling, bend detection.

I. INTRODUCTION

Subsea pipelines are the most efficient way to transport offshore oil and gas to land. The total length of subsea pipelines has rapidly increased while the seabed fossil energy resources have been highly explored. Subsea pipelines have a very high risk of fracture and leak due to the deformation and displacement caused by seabed moving, thermal expansion buckling, and spanning when the sediment below the pipeline is washed away by ocean currents [1]–[3]. Pipeline fracture and leakage will lead to substantial economic losses, serious environmental pollution, and even ecological disasters.

A bend is one of the most important causes of subsea pipeline fracture and is also an important warning sign before a fracture occurs. Pipeline bends may occur downward or upward during either spanning or buckling. Ocean currents can scour the soil underneath the pipeline to cause free spanning, where a segment of the pipeline becomes unsupported except at the two ends of the free span length [4], [5]. For a spanning pipeline that loses support below, the self-weight makes the pipeline bend downward. The span length will continuously increase as the current scours. The longer the span is, the more severe the pipeline bend is. If the bend stress exceeds the yield limit of the pipe steel, the pipeline will break. A buckling pipeline may bend upward or laterally. Subsea pipelines often buckle due to thermal expansion because the crude oil transported inside the pipeline is usually heated to a very high temperature to prevent condensation [6]–[8]. When the axial extension increases to a certain extent, overall vertical or lateral buckling may occur in the form of a sudden severe bend. If the pipeline is buried at a shallow depth, vertical buckling easily occurs, while if the soil on one side is soft, lateral buckling easily occurs. To repair and strengthen a bent pipeline in time to avoid fracture, it is necessary to monitor or detect in quasi real-time the subsea pipeline bend.

Typically, harsh environments and the difficulty of accessing underwater pipelines make the inspection and monitoring of subsea pipelines a challenging task [9], [10]. Underwater robots, such as ROVs and AUVs, can observe and find any

The associate editor coordinating the review of this manuscript and approving it for publication was Laxmisha Rai.

bending deformations of subsea pipelines through acoustic or optical imaging [11], [12]. However, due to the high deployment cost and long detection period, it is impossible for underwater robots to achieve the monitoring or quasi real-time detection of subsea pipeline bending. A distributed optical fiber [13]–[15] can monitor the pipeline bend by measuring the strain in real time. However, most subsea pipelines have no accompanying optical fiber because it is extremely difficult to lay optical fiber onto a subsea pipeline surface [16].

Interior pipeline inspection has the advantages of high efficiency and not being constrained by the external environment. There are two types of pipe detectors: cylindrical pipeline inspection gauges (PIGs) and spherical detectors (SDs). PIGs [17], [18] are widely used in land pipelines. However, because PIGs are bulky and contact the pipe wall tightly like a piston, they are susceptible to pipe deformation and bending. These phenomena can cause blockages and limit their application in subsea pipelines. The diameter of an SD [19], [20] is smaller than the pipe diameter, so the SD has the advantages of convenient deployment and low blockage risk. Through simulations and many field experiments, the passing ability of the SD, especially the ability to pass through vertical pipes, has been adequately verified [21]. In addition, versatile pipeline detection applications, such as 3D pipeline localization [22], pipeline inflection point and magnetic anomaly detection [23], pipeline inclination measurement [24], and vibration detection [25] for spanning pipelines, have fully demonstrated the robust detection ability of SDs and their advantage of quasi real-time detection. Therefore, the SD shows promise in the field of subsea pipeline detection.

In previous research, we found that the acceleration recorded by an SD rolling forward in the pipeline can indicate the rolling speed that is related to the pipeline inclination. When the SD can stably rotate around a fixed axis, its accelerometer output is more analytical and readable. This paper proposes using SDs to detect the downward bend of a spanning pipeline and the upward bend of a buckling pipeline. This paper will analyze the mathematical output model of an accelerometer as it rolls forward together with an SD, reveal the relationship between the pipeline bend and the acceleration characteristics of the SD, and provide a low-cost and high-efficiency method of using a SD to detect a pipeline bend. The accelerometer layout will be optimized via testing the influence of different arrangement angles and centrifugal distances of the accelerometer on the bend detection performance. Finally, experiments will be carried out to demonstrate that the SD can detect different degrees of upward and downward pipeline bends.

II. DETECTION PRINCIPLE

As shown in Figure 1 (a), an SD carrying a triaxial accelerometer is pushed by the flow and rolls forward in the pipeline. As the SD passes through the bend of a pipeline, it will successively go through uphill-downhill or downhill-uphill processes, and the recorded acceleration will thus contain

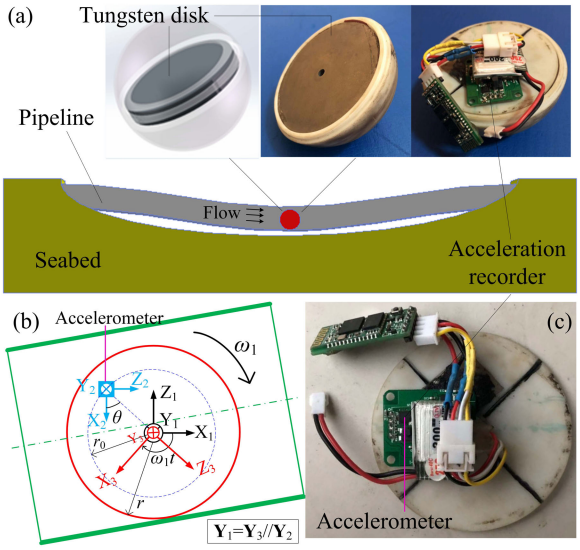

FIGURE 1. Detection process of subsea pipeline bend using an SD: (a) the SD is rolling inside a spanning and downward bent pipeline; (b) the coordinate frames of the accelerometer, the SD, and the pipeline; (c) picture of the acceleration recorder.

certain features. The pipeline bend is identified via the off-line signal processing of the acceleration recorded by the SD. There is a heavy tungsten disk on the middle plane of the SD, and the accelerometer is attached to the tungsten disk. The tungsten disk accounts for 90% of the SD's weight, so the mass of the SD is mainly distributed on the middle plane. The rotational inertia of the SD around the disk axis is much larger than that around other axes, so the SD can stably roll around the disk Y_3 that is parallel to one of the sensitive axes Y_2, as shown in Figure 1(b).

The pipeline coordinate system is denoted as O_1-$X_1Y_1Z_1$, the sensor coordinate system is denoted as O_2-$X_2Y_2Z_2$, and the SD coordinate system is denoted as O_3-$X_3Y_3Z_3$. O_1-$X_1Y_1Z_1$ moves but does not rotate with the SD, and its origin is at the SD center. The origin of frame O_3-$X_3Y_3Z_3$ is also at the center of the SD, but this frame moves and rotates together with the SD. Axis Y_3 is parallel to both Y_1 and Y_2. Assuming that the rotation angular frequency of the SD is $\omega_1 = 2\pi f_1$, the transformation matrix from frame O_3-$X_3Y_3Z_3$ to O_1-$X_1Y_1Z_1$ is as follows:

$$\mathbf{R}_{13} = \begin{bmatrix} \cos\omega_1 t & 0 & \sin\omega_1 t \\ 0 & 1 & 0 \\ -\sin\omega_1 t & 0 & \cos\omega_1 t \end{bmatrix} \tag{1}$$

Once the assembly of the SD is completed, the position and posture of the accelerometer relative to the SD is fixed, and the angle between the X/Z-axis of the accelerometer and the X/Z-axis of the SD is also fixed. Therefore, the transformation matrix from frame O_3-$X_3Y_3Z_3$ to O_2-$X_2Y_2Z_2$ is as follows:

$$\mathbf{R}_{32} = \begin{bmatrix} \cos\theta & 0 & -\sin\theta \\ 0 & 1 & 0 \\ \sin\theta & 0 & \cos\theta \end{bmatrix} \tag{2}$$

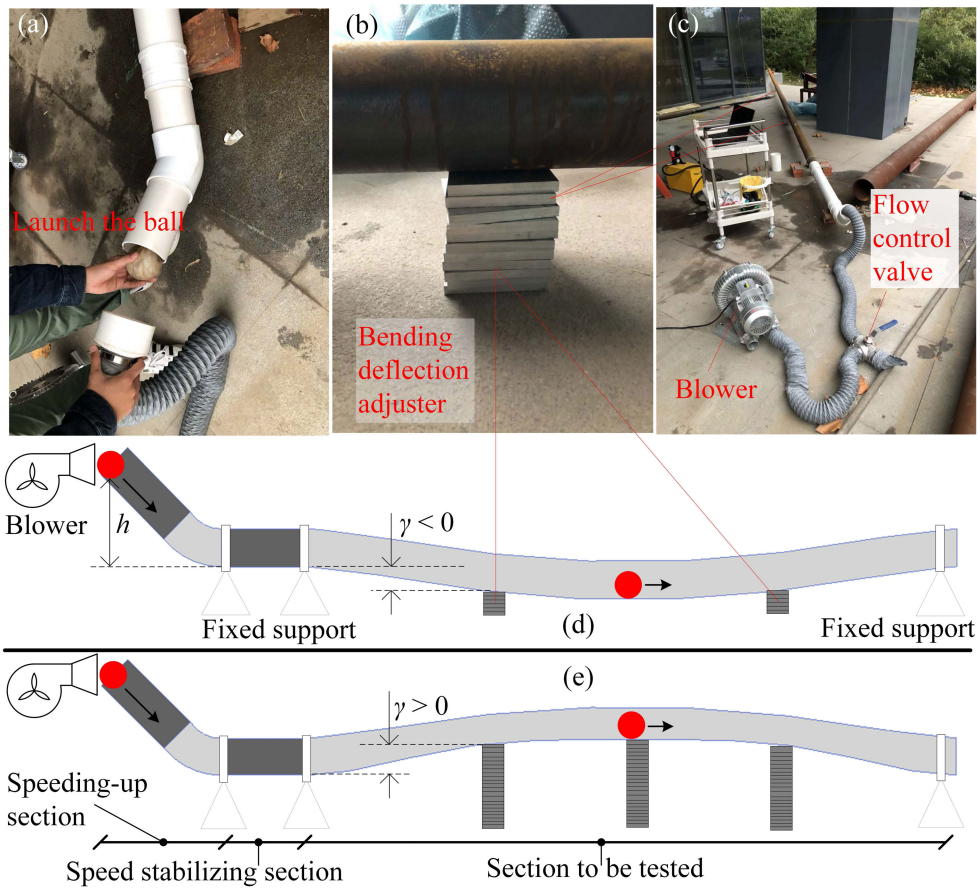

FIGURE 2. Experimental apparatus and method: (a)-(c): experimental pictures; (d) downward bend detection experiment, mimicking a spanning pipeline; (e) upward bend detection experiment, mimicking a buckling pipeline caused by thermal expansion.

θ is the angle between the X-axis of the accelerometer frame and the Z-axis of the SD frame and is also the angle between the Z-axis of the accelerometer frame and the X-axis of the SD frame. We can obtain:

$$\mathbf{R}_{12} = \mathbf{R}_{13}\mathbf{R}_{32} = \begin{bmatrix} \cos(\omega_1 t + \theta) & 0 & \sin(\omega_1 t + \theta) \\ 0 & 1 & 0 \\ -\sin(\omega_1 t + \theta) & 0 & \cos(\omega_1 t + \theta) \end{bmatrix} \quad (3)$$

The output of the accelerometer, $\mathrm{a} = (a_x, a_y, a_z)^T$, can be written as follows:

$$\begin{aligned} \mathbf{a} &= \mathbf{R_{21}}(0, 0, -g)^T + \mathbf{R_{23}}\left(0, 0, \omega_1^2 r_0\right)^T + \boldsymbol{\sigma}^T \\ &= \mathbf{R}_{12}^T(0, 0, -g)^T + \mathbf{R}_{32}^T\left(0, 0, \omega_1^2 r\right)^T + \boldsymbol{\sigma}^T \quad (4) \\ a_x &= \mathrm{g}\sin(\omega_1 t + \theta) + \sin\theta\omega_1^2 r_0 + \sigma_x \quad (5) \\ a_y &= \sigma_y \quad (6) \\ a_z &= -\mathrm{g}\cos(\omega_1 t + \theta) + \cos\theta\omega_1^2 r_0 + \sigma_z. \quad (7) \end{aligned}$$

where r_0 is the distance from the accelerometer to the rotating axis. The DC component is the centripetal acceleration. Formulas (5) - (7) indicate that the acceleration component along the sensitive axis that coincides with the rotation axis is zero, and the information related to rotation will be completely transferred to the other two sensitive axes. In addition, the amplitude of the AC component of the other two axes is the same and is not related to the rolling frequency ω_1, while the DC component is related to ω_1 and can also be affected by r_0 and θ. When the SD passes through the bent pipeline, the rolling velocity will change, leading to changes in the AC frequency and DC offset of the acceleration. r_0 and θ can affect the sensitivity of the DC component to the rolling speed, so the part layout requires careful design. Finally, a bend in a pipeline can be inferred by using the frequency of the AC component or the value of the DC component of either a_x or a_z.

III. EXPERIMENTS

The experimental apparatus is shown in Figure 2. A Φ105 mm$\times$T4 mm$\times$12 m steel pipe was supported at two ends for testing. An air pump was used to inject air into the pipe and push the SD to roll forward. A three-way valve was used to control the velocity of air flow in the pipe to adjust the driving force so that the SD can roll with a constant speed when the pipe does not bend. In each test, the SD entered

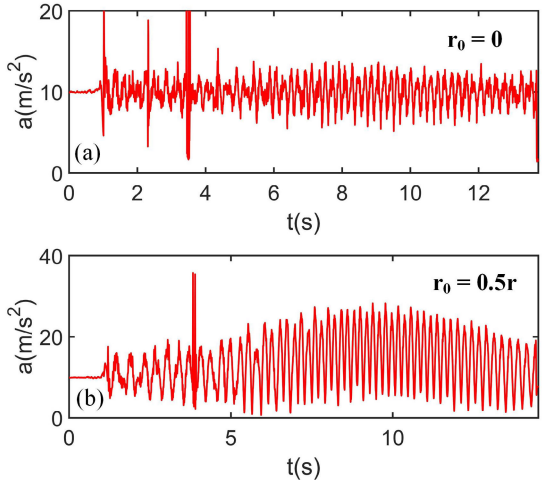

FIGURE 3. |a| measured by the SD with different r_0 inside a downward bent pipeline.

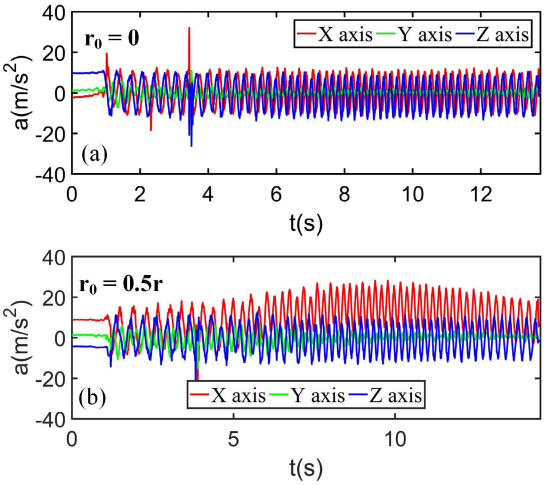

FIGURE 4. Acceleration components measured by the SD with different r_0 inside a downward bent pipeline.

the steel pipe from one end and rolled out from the other end. A 2 m PVC pipe was connected to the upstream of the steel pipe as a buffer to help the SD complete the process of accelerating before entering the steel pipe. The launch height h of the SD could be adjusted to make the entering speed approximately equal to the steady speed in the steel pipe to expedite the buffering process. An SD with different r_0 and θ was launched in the downward bending pipe many times to determine the proper installation position and posture of the accelerometer. The test results of different bending degrees were evaluated. An optimal installation configuration was adopted to test the detection performance of the SD for downward and upward bends with different deflections.

For the downward bend test, the steel pipe was supported at two ends high enough to make the pipe bend downward freely without touching the ground. Two stacks of aluminum blocks were padded below the pipe at the 1/3 and 2/3 positions to keep the steel pipe straight on the horizontal plane. The numbers of aluminum blocks at the two positions were simultaneously adjusted to change the extent of the bend, which is expressed by the deflection γ, as shown in Figure 2. When the steel pipe is freely bent, γ measures 5 cm under the current test conditions. The γ was gradually adjusted from 0 cm (horizontal and straight) to 5 cm (freely downward bend) with an interval of 1 cm, and the SD was launched to roll through the pipe with each value of γ, and it recorded the acceleration signals. For the upward bend test, three stacks of aluminum blocks were padded below the pipe at the 1/3, 1/2, and 2/3 positions. Three-point support can mimic the upward bend of a pipe similar to an actual bend. The bend feature was extracted from the recorded acceleration data to evaluate the bend detection performance of the SD.

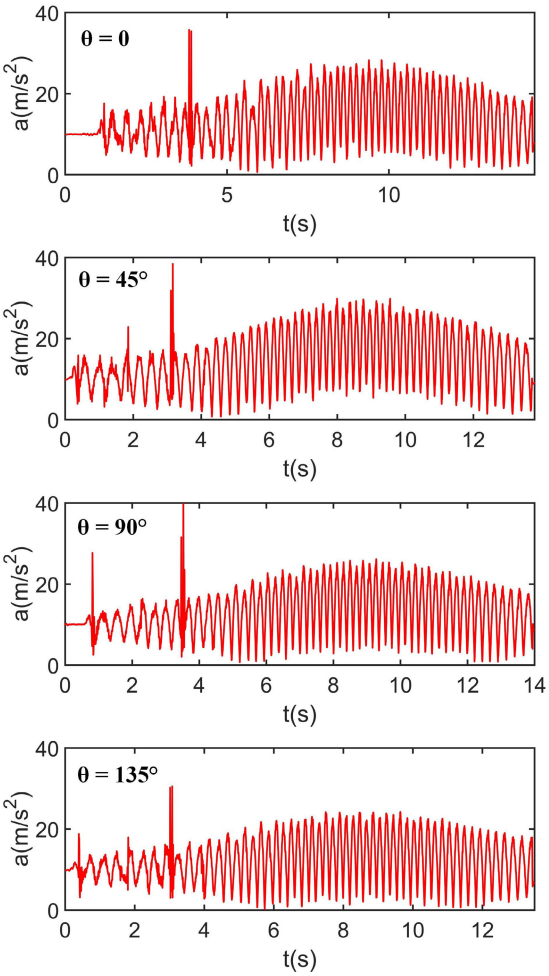

FIGURE 5. |a| measured by the SD with different θ inside a downward bent pipeline.

IV. RESULTS AND DISCUSSION

A. INFLUENCE OF DIFFERENT R_0 ON THE TEST RESULTS

The SD rolled through the downward bent pipe twice: the first time, the accelerometer was at the sphere center; for the second time, the accelerometer was not at the center. The two groups of acceleration signals are shown in Figures 3 and 4. Although the rolling speed of the SD inside a downward bent pipeline first increases and then decreases, whether the DC components a_x, a_z, and | a | can indicate the bend definitely

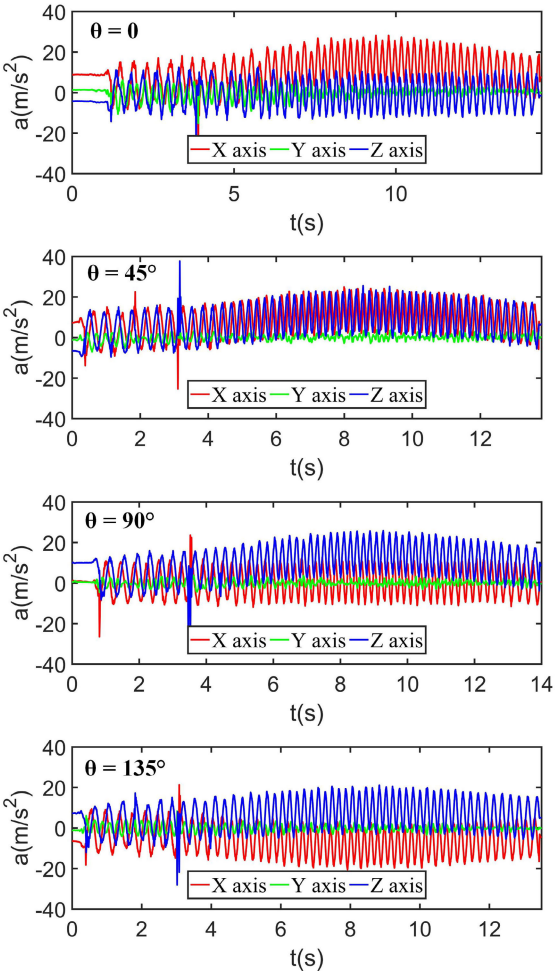

FIGURE 6. Acceleration components measured by the SD with different θ inside a downward bent pipeline.

depends on the value of r_0, which is the distance between the accelerometer and the sphere center. When the accelerometer is located at the center of the SD, $r_0 = 0$, the DC component is always 0 and cannot indicate the pipeline bend. When $r_0 \neq 0$, the pipeline bend can be easily identified by the DC component. These phenomena verify the correctness of formulas (5)-(7). Therefore, r_0 should be as large as possible to ensure that the DC component of the acceleration is large enough to sensitively detect the pipeline bend.

B. INFLUENCE OF DIFFERENT θ ON THE TEST RESULTS

θ has little effect on the DC component of the acceleration norm |a|, as shown in Figure 5, but it does have a noticeable effect on the DC subcomponent of each acceleration component a_x and a_z, as shown in Figure 6. When $\theta = 0°$, the DC component of a_z is 0, while the DC component of a_x is noticeable; in this case, the information of the pipe bend is completely included in a_x. When $\theta = 45°$, the DC components of a_x and a_z are equal, and the information of the pipe bend is incorporated into both of these two components; the a_x and a_z curves are bent in the same direction.

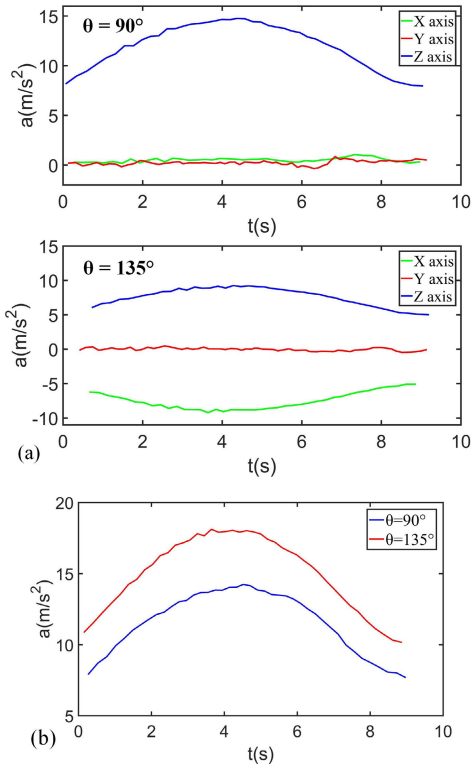

FIGURE 7. Feature extraction of pipeline bend: (a): DC subcomponent of each acceleration component when $\theta = 90°$ and $\theta = 135°$; (b) Difference of a_x and a_z's DC subcomponents when $\theta = 90°$ and 135°.

When $\theta = 135°$, the DC components of a_x and a_z are equal, and the information of the pipe bend is incorporated into both of these two components; the a_x and a_z curves are bent in the opposite directions. When $\theta = 90°$, the DC component of a_x is 0, while the DC component of a_z is noticeable; in this case, the information of the pipe bend is completely included in a_z. The form of the data when $\theta = 90°$ is similar to that when $\theta = 0°$. When $\theta = 135°$ and $\theta = 45°$, the shapes of the a_x and a_z components are similar, but the data curve is bent in the opposite direction.

The above test results are consistent with formulas (5) - (7). For pipeline bend detection, the two configurations of $\theta = 0°$ and $\theta = 90°$ are equivalent. The test result with $\theta = 135°$ is more recognizable than that with $\theta = 45°$. Either $\theta = 90°$ or $\theta = 135°$ should be used for bend detection, but which of these two has higher sensitivity must be determined. First, the DC subcomponents of a_z and a_x in the two configurations are extracted and plotted together in Figure 7 (a) for comparison, but it is difficult to evaluate the sensitivity from any single component. Then, the difference of the DC subcomponents of a_z and a_x when $\theta = 135°$ is calculated and compared with the DC component of a_z when $\theta = 90°$, and the results are shown in Figure 7 (b). It can be seen that the curve with $\theta = 135°$ is more curved than that with $\theta = 90°$. Therefore, the configuration of $\theta = 135°$ has higher sensitivity in pipeline bend detection. The following tests also adopt this configuration.

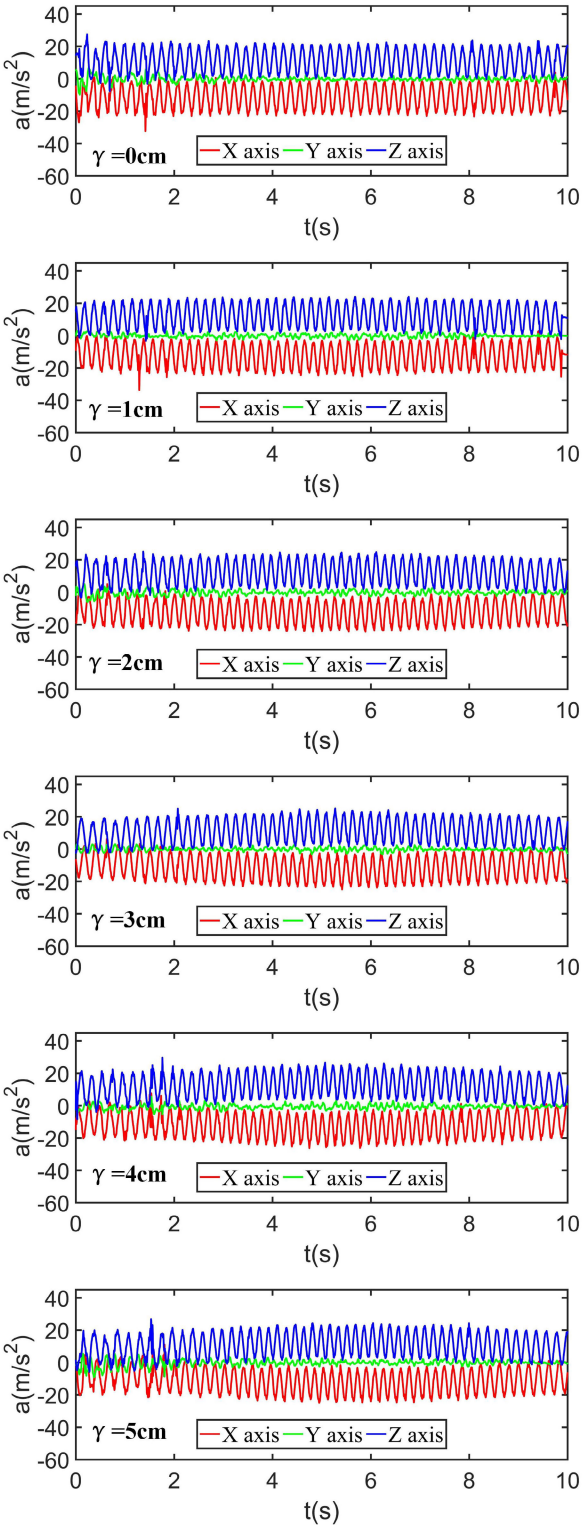

FIGURE 8. Raw rolling acceleration signals measured by the SD with $r_0 = 0.5r$ and $\theta = 135°$ when a spanning pipeline bends to different extents.

C. DETECTION RESULTS OF DOWNWARD BENDS WITH DIFFERENT EXTENTS

If the steel pipeline is more curved and bent, the change in the SD rolling velocity will be larger, and the DC component

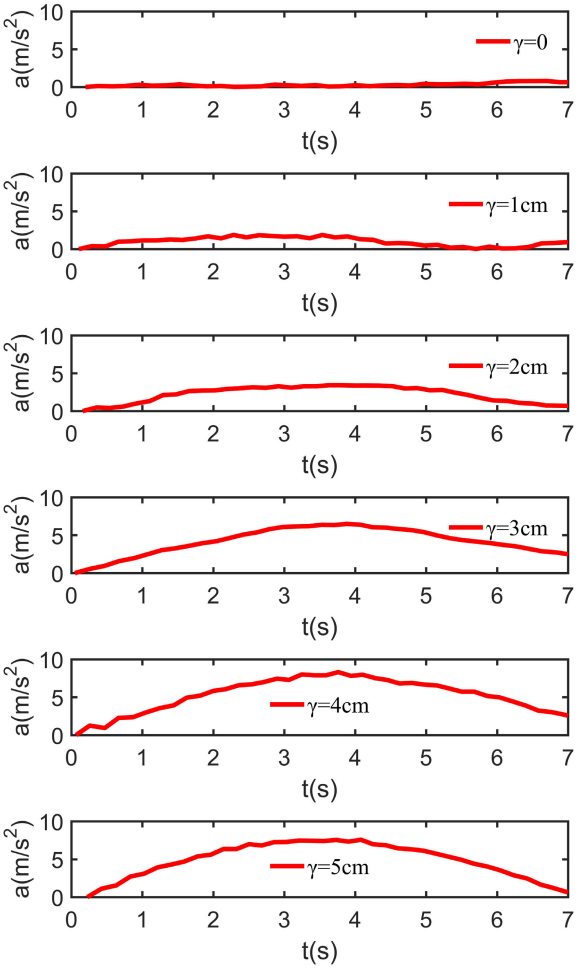

FIGURE 9. Differential DC characteristics of spanning pipeline bending with different extents when $r_0 = 0.5r$ and $\theta = 135°$.

of the acceleration data will thus have a more noticeable bend feature. To test the resolution of pipeline bend detection, the condition is set to be $r_0 = 0.5r$ and $\theta = 135°$, and the acceleration signals of a downward bent pipeline with different γ values are compared. The original data are shown in Figure 8. The pipeline does not bend when $\gamma = 0$ cm, and the DC component of acceleration data is close to zero. It can be seen that as γ increases from 0 cm to 5 cm, and the pipeline bends more severely, the DC component of the acceleration also increases. However, it is still difficult to distinguish the two adjacent bend extents from the original rolling acceleration signals.

To enhance the characteristics of the acceleration signal related to the pipeline bend, the difference of the DC subcomponents of a_x and a_z is extracted and shown in Figure 9. The differential DC subcomponent noticeably increases as γ increases, and the consequence of γ changing by 1 cm for a 12 m pipeline can be determined. The bend detection resolution is higher when using the DC subcomponent than when using the original rolling signals. Therefore, in field pipeline bend detection, the original data can be used to

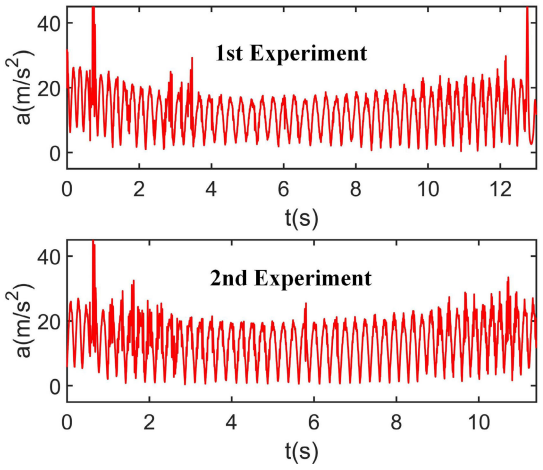

FIGURE 10. |a| measured by the SD inside a buckling pipeline that bends upward, repeated twice.

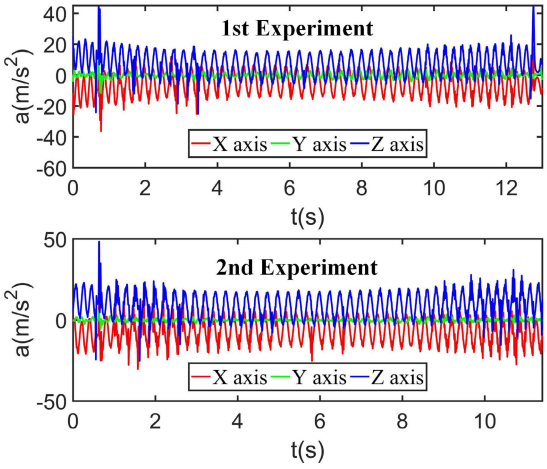

FIGURE 11. Three acceleration components measured by the SD inside a buckling pipeline that bends upward, repeated twice.

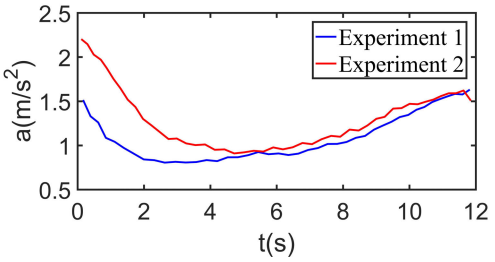

FIGURE 12. Differential DC subcomponent for a buckling pipeline that bends upward, repeated twice.

identify a severe bend, while for a slight bend, it is necessary to extract the DC subcomponent to enhance the sensitivity and resolution.

D. DETECTION RESULTS OF UPWARD BENDS WITH DIFFERENT EXTENTS

An upward bend can be formed when pipeline buckling occurs due to thermal extension. The occurrence of pipeline buckling is binary; that is, a straight pipeline can suddenly switch into a buckling state without undergoing a transition process of different bend extents. Therefore, a detection experiment on a pipeline that was noticeably bent upward was carried out by using the SD with the configuration of $r_0 = 0.5r$ and $\theta = 135°$. The acceleration data when the SD rolled through the upward bent pipeline twice were recorded to verify the stability of the detection method. The original data are shown in Figure 10 and Figure 11, and the corresponding DC component curves are shown in Figure 12. It can be seen that the bend direction of the rolling acceleration for an upward bent pipeline is opposite to that for a downward bent pipeline. Therefore, this result indicates that the pipe bends down if the DC component is a convex curve, while the pipe bends up if the DC component is a concave curve.

V. CONCLUSION

(1) Low blockage risk and rolling features characterize the SD competent that detects the vertical bends in subsea pipelines in quasi-real-time by recording and processing the rolling acceleration signals. If the DC component is a convex curve, then the pipe is bent downward, and there is spanning or seabed settling; if the DC component is a concave curve, then the pipe is bent upward, and there is vertical buckling.

(2) The mass of the SD should be distributed as much as possible in the disc area at the center to make the SD roll around a fixed axis. To enhance the bend detection sensitivity, one of the sensitive axes of the accelerometer should be parallel to the rotation axis, the included angle between any one of the other two axes and the line of sight from the rotation center to the accelerometer should be 135°, and the accelerometer should be as far from the rotation axis as possible.

(3) A noticeable pipeline bend can be directly identified from the original raw acceleration data. When the bend extent is very small, it is necessary to extract the DC component from the acceleration data and then sum the absolute values to improve the detection sensitivity. The bend detection resolution can reach 1 cm for a 12 m pipeline.

REFERENCES

[1] A. Zakeri, "Review of state-of-the-art: Drag forces on subsea pipelines and piles caused by landslide or debris flow impact," *J. Offshore Mech. Arctic Eng.-Trans. Asme*, vol. 131, no. 1, pp. 403–410, Feb. 2009.
[2] L. Cheng, K. Yeow, Z. Zang, and F. Li, "3D scour below pipelines under waves and combined waves and currents," *Coastal Eng.*, vol. 83, pp. 137–149, Jan. 2014.
[3] J. Cai, X. Jiang, and G. Lodewijks, "Residual ultimate strength of offshore metallic pipelines with structural damage—A literature oreview," *Ships Offshore Struct.*, vol. 12, no. 8, pp. 1037–1055, Nov. 2017.
[4] M. M. Shabani, A. Taheri, and M. Daghigh, "Reliability assessment of free spanning subsea pipeline," *Thin-Walled Struct.*, vol. 120, pp. 116–123, Nov. 2017.
[5] A. A. Shittu, F. Kara, A. Aliyu, and O. Unaeze, "Review of pipeline span analysis," *World Eng.*, vol. 16, no. 1, pp. 166–190, Feb. 2019.
[6] Y. Chai and T. Zhao, "Probability of upheaval buckling for subsea pipeline considering uncertainty factors," *Ships Offshore Struct.*, vol. 13, no. 6, pp. 630–636, Aug. 2018.
[7] Z. Liang, X. Lu, and J. Zhang, "Thermal vertical buckling of surface-laid submarine pipelines on a sunken seabed," *Ocean Eng.*, vol. 173, pp. 331–344, Feb. 2019.
[8] X. Zhang and C. G. Soares, "Lateral buckling analysis of subsea pipelines on nonlinear foundation," *Ocean Eng.*, vol. 186, Aug. 2019, Art. no. 106085.

[9] P. Davis and J. Brockhurst, "Subsea pipeline infrastructure monitoring: A framework for technology review and selection," *Ocean Eng.*, vol. 104, pp. 540–548, Aug. 2015.
[10] M. Ho, S. El-Borgi, D. Patil, and G. Song, "Inspection and monitoring systems subsea pipelines: A review paper," *Struct. Health Monitor.*, vol. 19, no. 2, pp. 606–645, Mar. 2020.
[11] O. Ola, "ROV based survey: A new, more effective approach," in *Proc. Annu. Offshore Technol. Conf.*, vol. 4, 2016, pp. 3070–3081.
[12] V. H. Fernandes, A. A. Neto, and D. D. Rodrigues, "Pipeline inspection with AUV," in *Proc. IEEE/OES Acoust. Underwater Geosci. Symp. (RIO Acoustics)*, Jul. 2015, pp. 1–5.
[13] N. Xiuyi and Y. Yongchun, "Long-term monitoring system of submarine pipeline vibration based on fiber grating sensor technology," in *Proc. Int. Offshore Polar Eng. Conf.*, 2018, pp. 230–237.
[14] D. Maraval, R. Gabet, Y. Jaouen, and V. Lamour, "Dynamic optical fiber sensing with Brillouin optical time domain reflectometry: Application to pipeline vibration monitoring," *J. Lightw. Technol.*, vol. 35, no. 16, pp. 3296–3302, Aug. 15, 2017.
[15] X.-F. Zhao, L. Li, Q. Ba, and J.-P. Ou, "Scour monitoring system of subsea pipeline using distributed Brillouin optical sensors based on active thermometry," *Opt. Laser Technol.*, vol. 44, no. 7, pp. 2125–2129, Oct. 2012.
[16] W. Ruijuan, Z. Baikang, and T. Qinchang, "Application of optical fiber sensing technology in operation monitoring of submarine pipeline," *China Water Transp.*, vol. 17, no. 5, pp. 303–306, 2017.
[17] J. Quarini and S. Shire, "A review of fluid-driven pipeline pigs and their applications," *Proc. Inst. Mech. Eng., E, J. Process Mech. Eng.*, vol. 221, no. 1, pp. 1–10, Feb. 2007.
[18] H. S. Han, J. J. Yu, C. G. Park, and J. G. Lee, "Development of inspection gauge system for gas pipeline," *KSME Int. J.*, vol. 18, no. 3, pp. 370–378, Mar. 2004.
[19] F. Richard and C. Muthu, "SmartBall: A new approach in pipeline leak detection, in Proc," in *Proc. Biennial Int. Int. Pipeline Conf.*, vol. 2, 2009, pp. 117–133.
[20] S. X. Guo, S. L. Chen, X. J. Huang, and T. S. Xu, "Design of a spherical leak detector for submarine oil pipelines," *Appl. Mech. Mater.*, vol. 709, pp. 460–464, Dec. 2014.
[21] S. Guo, S. Chen, X. Huang, Y. Zhang, and S. Jin, "CFD and experimental investigations of drag force on spherical leak detector in pipe flows at high Reynolds number," *Comput. Model. Eng. Sci.*, vol. 101, no. 1, pp. 59–80, 2014.
[22] X. Huang, S. Chen, S. Guo, T. Xu, Q. Ma, S. Jin, and G. S. Chirikjian, "A 3D localization approach for subsea pipelines using a spherical detector," *IEEE Sensors J.*, vol. 17, no. 6, pp. 1828–1836, Mar. 2017.
[23] H. Xinjing, C. Guanren, Z. Yu, L. Jian, X. Tianshu, and C. Shili, "Inversion of magnetic fields inside pipelines: Modeling, validations, and applications," *Struct. Health Monitor.*, vol. 17, no. 1, pp. 80–90, Jan. 2018.
[24] Z. Yu, X. Yameng, H. Xinjing, L. Jian, and C. Shili, "Pipeline inclination measurements based on a spherical detector with magnetic proximity switches," *IEEE Access*, vol. 6, pp. 39936–39943, 2018.
[25] G. Lin, Z. Zhoumo, H. Xinjing, L. Jian, and C. Shili, "Vibration detection of spanning subsea pipelines by using a spherical detector," *IEEE Access*, vol. 7, pp. 7001–7010, 2019.

GUO LIN received the B.E. degree from the Harbin Institute of Technology, in 2010, and the M.E. degree from Sun Yat-sen University, in 2014. He is currently pursuing the Ph.D. degree with Tianjin University (TJU). His research interest is in span inspection of subsea pipelines.

ZENG ZHOUMO received the Ph.D. degree from Tianjin University (TJU), in 1993. He is currently a Professor with TJU. He is also the Dean of the School of Precision Instrument and Opto-Electronics Engineering. His research interests are in detection technology and instrument, system integration and intellectualization, and MEMS.

HUANG XINJING received the B.S. and Ph.D. degrees from Tianjin University (TJU), in 2010 and 2016, respectively. He is currently an Assistant Professor with TJU. His research interest is in pipeline damage detections.

LI MINGZE, photograph and biography not available at the time of publication.

FENG HAO, photograph and biography not available at the time of publication.

LI JIAN received the B.E., M.E., and Ph.D. degrees from Tianjin University (TJU), in 1994, 1997, and 2000, respectively. He is currently a Professor with TJU. His research interests include pipeline leak detection and pipeline safety warning.

RUI XIAOBO, photograph and biography not available at the time of publication.